Clusters on the Edge: The Interface Between Galaxy Cluster Outskirts and Large-Scale Filaments

[1,2]G.E. Alvarez, [1]S.W. Randall, [1]H. Bourdin, [1]C. Jones, [2]K. Holley-Bockelmann, Y. Su[3]
[1]Harvard-Smithsonian Center for Astrophysics, [2]Vanderbilt University,[3]University of Kentucky

Introduction

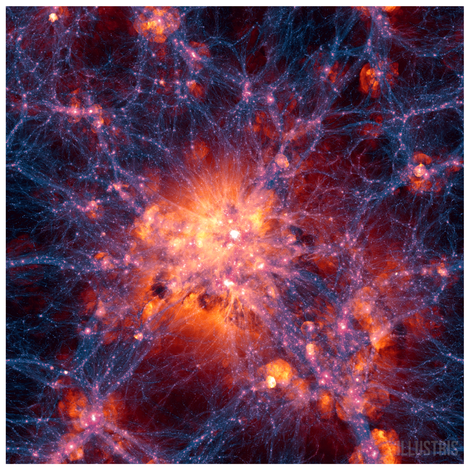

Fig.1 Snapshot from the Illustrious simulation highlighting galaxy clusters and large scale filaments.

We see in cosmological simulations (Figure 1) and observational data (e.g., SDSS) that there is a large scale filamentary structure in the universe in which most galaxies and galaxy clusters are found. Galaxy clusters are the nodes, and the largest known structures in the universe and can therefore be used to constrain cosmology. One important assumption is that the galaxy clusters are in hydrostatic equilibrium. However, there are deviations from hydrostatic equilibrium near the cluster outskirts, where they are thought to interface with large-scale structure filaments.

There are also “missing baryons” in the local universe; we don’t see the amount of baryons we expect based on big bang nucleosynthesis and high redshift observations. Observational evidence of the existence of filamentary structure thus far has come from the spatial distribution of galaxies and galaxy clusters observed in large surveys. These filaments are theorized to contain most of the missing baryons that don’t reside in galaxies or in the ICM, although *Lynx* and *Athena* will help determine how much resides in the intergalactic medium (IGM). The missing baryons are theorized to be contained in a warm hot intergalactic medium (WHIM) with kT <1 keV and n_e < 10^{-5} cm^{-3}. Thus far there exist few reports of direct observations of the dense tail of WHIM (Werner+08, Bulbul+16), namely where the WHIM interfaces with cluster emission.

The Abell 3391/Abell 3395 Intercluster Filament: Early Stage Cluster Merger

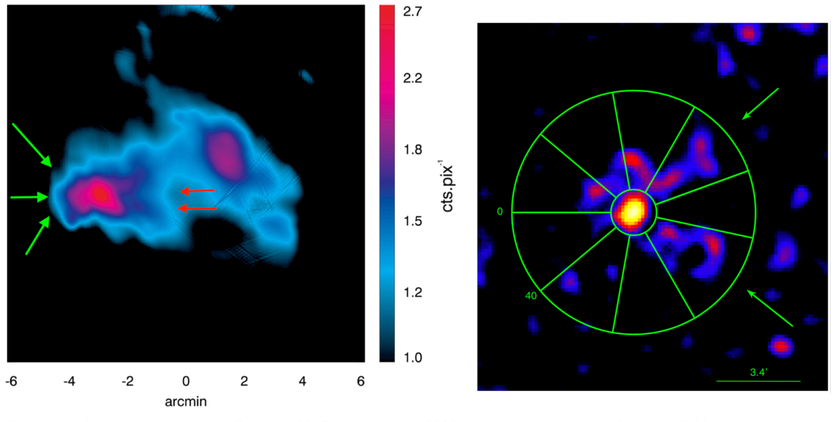

Fig 1. Left: Curvlet denoised (see Bourdin+2015 and Candes+2000 for more details) at the 3σ level *XMM-Newton* image of ESO-161. The colorbar is counts per pixel. The green arrows indicate the leading eastward edge and the red arrows indicate the possible downstream edge. Right:*Chandra* image from Figure 2 (Right). The overlaid azimuthal region is used for the surface brightness profile not shown here. The arrows indicate where the two potentially stripped gas tails are located. We also find that the galaxy group ESO-161 is most likely undergoing rem pressure stripping in the filamentary region.

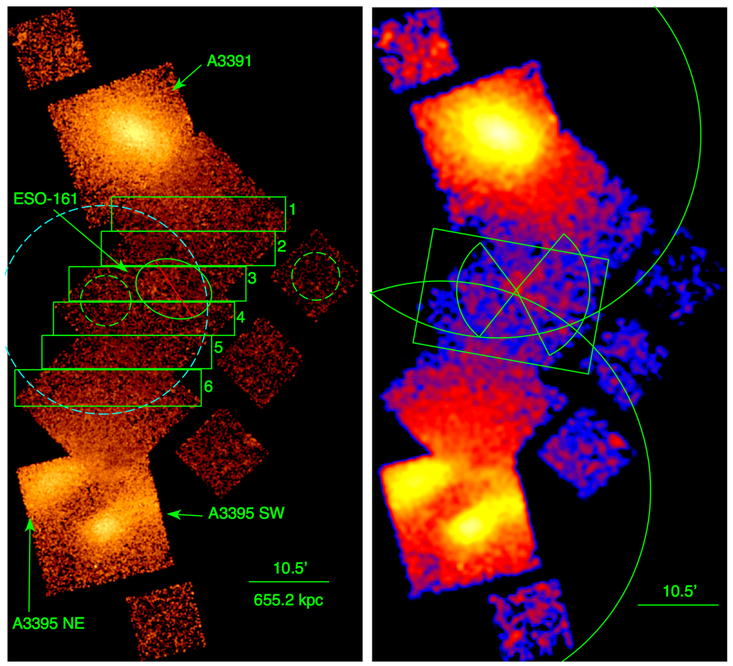

Fig 2. Left: The background-subtracted, exposure-corrected mosaic *Chandra* image of A3391, A3395, and the intercluster filament is shown in the 0.3-7.0 keV energy band and smoothed by a 12” Gaussian. The boxes denote regions used for the temperature profile of the filament shown in Figure 4. The excluded region, marked by the ellipse and red line, contains the galaxy group ESO-161. The green dashed circular region to the east of ESO-161 is used for local background modeling for the group temperature measurement. The green dashed circular region to the west on ACIS-I6 is used for background in *Chandra* spectral analyses. Right: Same as left but smoothed by a 40” Gaussian to highlight the intercluster filament emission. Spectra extracted from the green box region were used to estimate the global temperature and density of the filament. The northern and southern circles are r_{200} for A3391 and A3395 respectively. The wedges are used to derive the surface brightness profile of the group. The system has a mean redshift of z=0.053. We find a global filament temperature kT=$4.45_{-0.55}^{+0.89}$ keV, electron density n_e=$1.08^{+0.06}_{-0.05}$ x 10^{-4} cm^{-3}, and gas mass M_{gas} = $2.7^{+0.2}_{-0.1}$ x 10^{13} M$_\odot$ assuming a cylindrical geometry for the filament, with a length of 0.7 Mpc and a radius of 0.45 Mpc. Our measurement is for a cylinder oriented in the plane of the sky. We find that the ICM gas from the sub clusters is being tidally pulled into the intercluster filament as part of the early stages of a merger.

Ongoing Work: A possible Pre-Merger shock in the Abell 399/Abell 401 Intercluster Filament

The Abell 98 Intercluster Filament

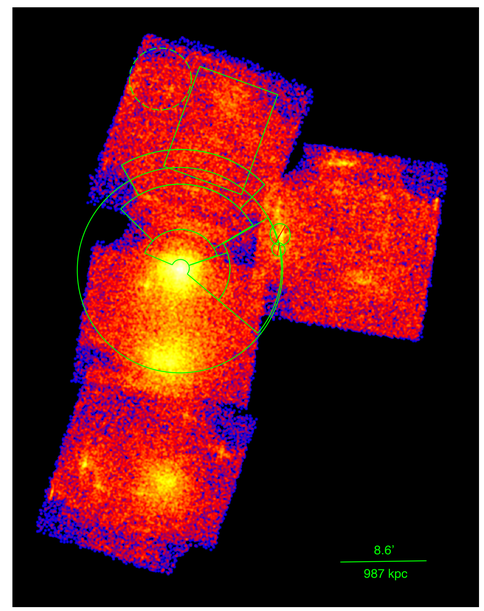

Fig 4. The background subtracted *Suzaku* mosaic image of Abell 98 (A98) is shown above. A98 consists of three sub clusters aligned along a large-scale putative intercluster filament. The circular region shows r_{200} for A98N.The dashed circular region is used for a local background spectrum. The sectors to the north and the west of A98N are used to investigate the thermodynamic state of the putative filament axis as compared to off axis to investigate self-similarity azimuthally. The box region to the north is used to measure the temperature and density (kT~1.55 kev ; n_e ~ 6.6 x 10^{-5} cm^{-3}) of the putative filamentary structure to the north of the system. A98N has a measured temperature of T_{500}=2.8 keV, and is the hottest sub cluster in this system.

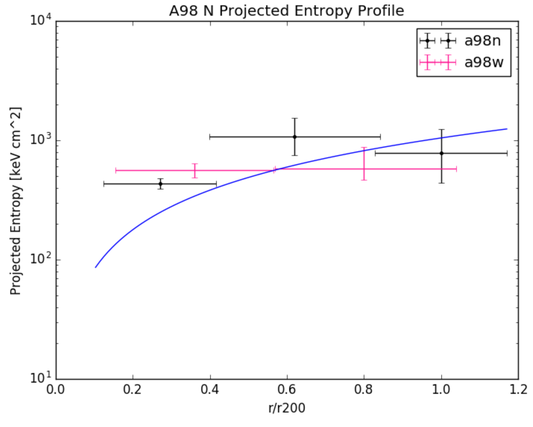

Fig 5. The projected entropy profiles are shown above for the sectors to the north (black) and west (pink) in Figure 4. The blue line is the self-similar prediction from pure gravitational collapse. A98N agrees with the SS prediction from Voit+05 (blue line) azimuthally. This measurement is in agreement with the prediction that lower mass clusters more closely follow SS than higher mass clusters made by Bulbul+16.

References

Bulbul, E., Randall, S.W., Bayliss, M., et al. 2016, ApJ, 818, 131
Bourdin, H., Bijaoui, A., Sauvageot, J.L., Belsole, E., & Slezak, E. 2005, Advances in Space Research, 36, 65
Bourdin, H., Mazzotta, P., Markevitch, M., Giacintucci, S., & Brunetti, G. 2013, ApJ, 764, 82
Candes, E., Donoho, D., Ann. Statist. Volume 30, Number 3 (2002), 784-842.
Smee, S.A., Gunn, J.E., Uomoto, A., et al. 2013, AJ, 146, 32
Tittley, E.R., & Henriksen, M. 2001, ApJ, 563, 673
Werner, N., Finoguenov, A., Kaastra, J. S., et al. 2008, A&A, 482, L29
Vogelsberger, M., Genel, S., Springel, V., et al. 2014, MNRAS, 444, 1518
Voit, G.M., Kay, S.T., & Bryan, G.L.\2005, MNRAS, 364, 909
ZuHone, J.A., Biffi, V., Hallman, E.J., et al. 2014, arXiv:1407.1783